Dynamical Simulations of Lattice QCD

K. Jansen, S. Schaefer, H. Simma, R. Sommer

published in

NIC Symposium 2016
K. Binder, M. Müller, M. Kremer, A. Schnurpfeil (Editors)

Forschungszentrum Jülich GmbH,
John von Neumann Institute for Computing (NIC),
Schriften des Forschungszentrums Jülich, NIC Series, Vol. 48,
ISBN 978-3-95806-109-5, pp. 39.
http://hdl.handle.net/2128/9842

Dynamical Simulations of Lattice QCD

Karl Jansen, Stefan Schaefer, Hubert Simma, and Rainer Sommer

John von Neumann Institute for Computing, DESY, Platanenallee 6, 15738 Zeuthen
E-mail: {karl.jansen, stefan.schaefer, hubert.simma, rainer.sommer}@desy.de

1 Introduction

Lattice calculations of Quantum Chromodynamics (QCD) are continuously becoming more realistic. Where Ukawa[1] famously concluded only fourteen years ago that simulations including two physically light sea quarks are basically impossible even with today's computers, algorithmic developments over the last years have changed this situation drastically. Nowadays up and down quark masses light enough to control the chiral extrapolation reliably are standard and also the sea quark effects of strange (and charm) quark are included.

Modern lattice simulations are an intricate interplay between a large variety of numerical methods on one side and the computer hardware on the other side. The main areas of progress have been the solvers used for the Dirac equation, fermion determinant factorisations and better integrators for the molecular dynamics which is at the heart of most algorithms used for QCD simulations.

In lattice QCD simulations the path integral is computed via a Markov Chain Monte Carlo method. In virtually all projects with dynamical fermions a variant of the Hybrid Monte Carlo algorithm is employed to generate the Markov chain, where the fields are updated using molecular dynamics. But there is considerable freedom in how to include the fermion determinant into the simulation. Factorisations[2,3] of this determinant have been essential in the progress of recent years, being successful in particular together with improved integrators of the molecular dynamics[4].

The solution of the Dirac equation constitutes the most computer time consuming element of simulations with fermions. The dramatic speedup for small fermion mass due to locally deflated solvers[5,6] has therefore had a significant impact on what is possible in the simulations. These algorithms have practically eliminated the increase in cost of the solution as the quark mass is lowered.

1.1 Autocorrelations

One of the main difficulties of Markov Chain Monte Carlo is the presence of autocorrelations: subsequent field configurations depend on previous ones and one essential requirement of a correct simulation is that the whole chain is much longer than the modes decorrelating most slowly.

In the study of the autocorrelations it has also become clear that significantly more statistics is required to reach precision results than previously thought. In particular observables constructed from smoothed gauge fields[7] turned out to be particularly sensitive to these long autocorrelations.

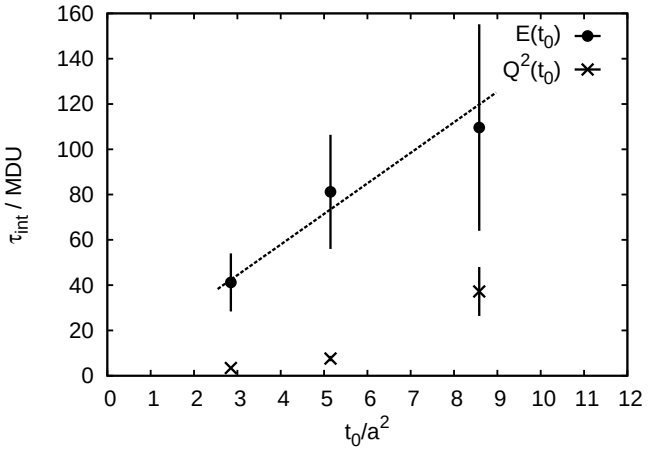

Figure 1. Scaling of the autocorrelation times of the action density E constructed from smoothed links and the topological charge Q with the lattice spacing a. The results are from the CLS 2+1 simulations using open boundary conditions. For E we observe scaling compatible with the theoretical expectation with a dynamical critical exponent of 2. There is no abnormal slowing down of the charge observed.

Finally, in the standard setup with periodic boundary conditions in space and time a dramatic critical slowing down of the algorithms has been observed[8], i.e. lowering the lattice spacing the number of update steps to reach an independent configuration in the Markov chain needed to be increased drastically. This was due to topological modes which need more and more time to decorrelate. This topological freezing is a property of the continuum theory which exhibits disconnected sectors in field space labelled by an integer topological charge.

A way out is to use open boundary conditions in time[9]. This avoids the sector formation in the continuum and avoids the presence of exceptionally slow modes in the Markov chain. These boundary conditions have therefore been adopted in the CLS simulations described below[10]. In Fig. 1 it is demonstrated that in simulations with open boundary conditions no dramatic slowing down is observed, even for quantities know for their sensitivity to slow modes.

2 Status of Dynamical Simulations

By their nature, three principal effects have to be controlled in simulations of lattice QCD: the effect of the finite lattice spacing a, the finite size of the box L and the unphysical quark masses. Furthermore also the consequences of the finite computer time available, and therefore a limited statistics of the Monte Carlo estimates, including the problem of the autocorrelations.

In these simulations, a compromise has to be found between the prominance of these various sources of systematic error. For example at fixed physical volume smaller light quark masses will lead to larger volume effects. Equally smaller lattice spacing will lead to longer autocorrelations – due to the critical slowing down of the algorithms – and therefore

ensemble	β	κ_c	$a\mu_\ell$	L/a	N_τ	$N_{\rm conf}$	τ	$\tau_{\rm int}(P)$
cA2.09.48	2.10	0.13729	0.0009	48	6900	2950	1	15(6)
cA2.30.24	2.10	0.13730	0.0030	24	3400	1300	1	3.2(8)
cA2.60.24	2.10	0.13730	0.0060	24	9000	4000	1	3.8(6)
cA2.60.32	2.10	0.13730	0.0060	32	11840	5350	1	2.9(5)

Table 1. The $N_{\rm f} = 2$ ETMC ensembles, all of which have temporal extent $T = 2L$ with L/a the spatial lattice extend. In addition we give the total number of trajectories N_τ, the number of thermalised configurations $N_{\rm conf}$ and the HMC trajectory length τ and the integrated autocorrelation time of the plaquette $\tau_{\rm int}(P)$.

observable	*cA2.09.48*	*cA2.30.24*	*cA2.60.24*	*cA2.60.32*
$aM_{\pi^\pm}$	$0.06196(09)(^{+12}_{-05})$	$0.1147(7)(^{+4}_{-7})$	$0.15941(38)(^{+15}_{-21})$	$0.15769(26)(^{+15}_{-14})$
$aM_{\pi^{(0,c)}}$	$0.1191(05)(^{+07}_{-10})$	$0.1541(13)(^{+05}_{-05})$	$0.18981(61)(^{+21}_{-25})$	$0.18840(44)(^{+46}_{-29})$
aM_{π^0}	$-^\dagger$	$0.09(1)^\star$	$0.11(2)^\star$	$0.13(2)^\star$

Table 2. The splitting between the charged and the neutral pion is a discretisation effect for twisted-mass fermions. In the new simulations it is much reduced compared to the previously used formulation. †: For *cA2.09.48*, disconnected diagrams have not been computed yet. $\star$: For the full neutral pion, a study of systematic effects from excited states was not possible due to the poor signal.

require increased length of the simulations.

In the following we will present two sets of such simulations: one by the ETM collaboration using twisted mass fermions, one by CLS with non-perturbatively improved Wilson fermions. Some of the choices of these simulations are similar, some also different and therefore allow for complementary checks concerning the control of systematic effects.

2.1 ETMC

Along with the $N_{\rm f} = 2 + 1 + 1$ simulations pursued by the European Twisted Mass collaboration (ETMC) in recent years, there has been a renewed interest in $N_{\rm f} = 2$ flavour simulations[11]. The leading discretisation effects of twisted mass fermions at maximal twist come always at $\mathrm{O}(a^2)$, but by adding the clover term with a suitably tuned coefficient, their magnitude could be reduced.

The simulation parameters are summarised in Tab. 1. As can be seen from the table, these simulations are so far restricted to one lattice spacing and relatively small volume ($m_\pi L \approx 3$ at the physical point), however, varying the lattice size L allows to study the volume effects and give estimates for these effects.

The main effect of the reduction of discretisation effects can be seen in the difference between the mass of the neutral and the charged pion. Where this has been quite noticeable in previous simulations without the clover term, the effect is now significantly reduced as can be seen from the results in Tab. 2.

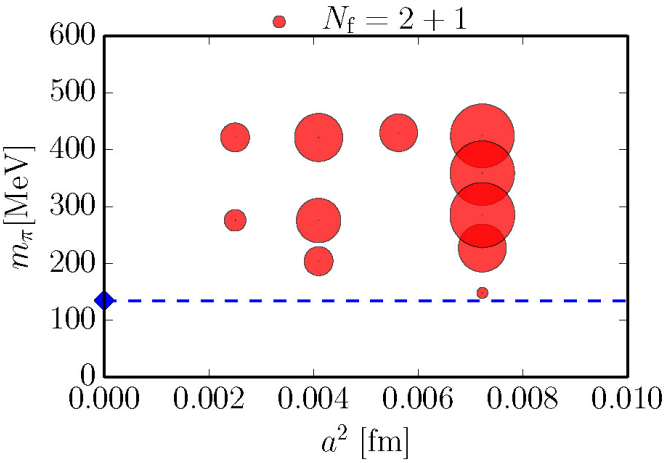

Figure 2. Lattice spacing a and pion mass m_π of the CLS 2+1 ensembles. The size of the circle is proportional to the number of independent gauge field configurations. The blue diamond indicates the physical point.

2.2 CLS

The Coordinated Lattice Simulations (CLS) have a programme to simulate $N_\mathrm{f} = 2 + 1$ flavours of non-perturbatively improved Wilson fermions. The project started in 2013 and by now has generated lattices at four different lattice spacings between 0.085 fm and 0.05 fm[12]. Lattice spacing and pion mass of these ensembles are visualised in Fig. 2, from which it becomes clear that the control over both, the chiral and the continuum limit is an essential part of this project. Both can bring significant corrections with respect to the lattice results. An example of this is given in Fig. 3 where the product of the pion decay constant with the gluonic scale parameter t_0 defined through the Wilson flow[7] is displayed. As we can see, the accuracy which can be reached in such a quantity is on the level of 1%.

The extrapolation towards the continuum limit agrees with leading scaling violations of $\mathrm{O}(a^2)$, as expected for this non-perturbatively $\mathrm{O}(a)$ improved theory. From the plot it is also obvious that only the fine lattices used here can lead to such a 1% accuracy – the points at 0.085 fm and 0.065 fm being $\mathrm{O}(5\%)$ away from the continuum result.

Also the chiral corrections are well under control as can be seen from Fig. 4. We show

$$f_{\pi\mathrm{K}} = \frac{2}{3}(f_\mathrm{K} + \frac{1}{2} f_\pi) \tag{1}$$

along the line of constant sum of quark masses $m_\mathrm{u} + m_\mathrm{d} + m_\mathrm{s}$. In particular in comparison to Fig. 3 it becomes clear that chiral and continuum extrapolations are equally important and to reach per cent level accuracies it is pivotal to control both at a high level of accuracy. It is remarkable that in the full range of quark masses, next-to-leading order chiral perturbation theory describes the effect to the 20% level.

With these lattices the foundation of a large variety of projects has been laid which are currently pursued in a number of European groups.

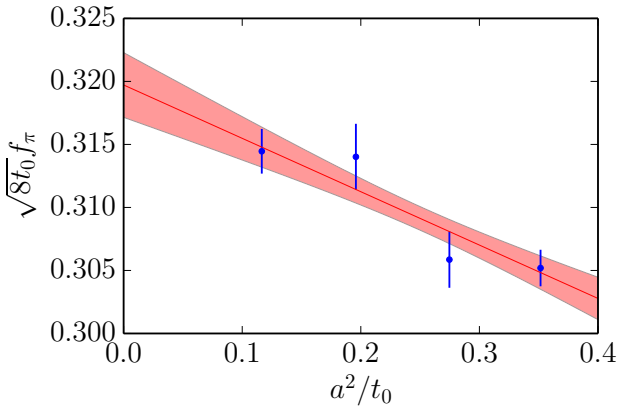

Figure 3. Continuum extrapolation of the dimensionless product $f_\pi\sqrt{8t_0}$ of the pseudoscalar decay constant f_π and the gluonic scale t_0 along the line $m_\pi = m_{\rm K} \approx 420$ MeV. Fine lattices are needed to reach a per cent level result.

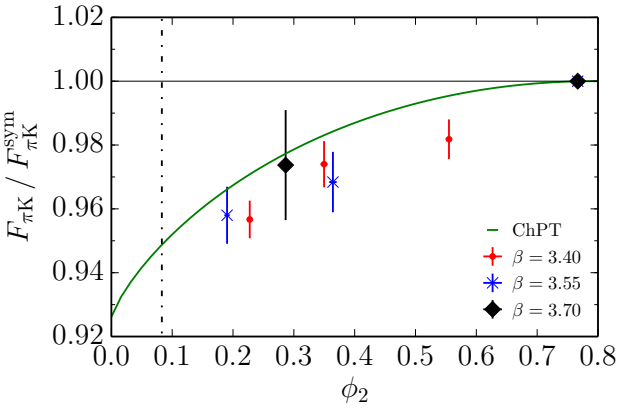

Figure 4. Chiral extrapolation of $f_{\pi{\rm K}} = \frac{2}{3}(f_{\rm K} + \frac{1}{2}f_\pi)$ along the line of constant sum of quark masses $m_{\rm u} + m_{\rm d} + m_{\rm s}$.

3 Anomalous Magnetic Moments

One particular result of the ETMC simulations described above are hadronic contributions to anomalous magnetic moments of the leptons, which give the deviation of Dirac's leading order value of the magnetic moment of a fermion $g = 2$. Hadronic contributions are the dominant source of uncertainty in the comparison of the quantum field theory prediction of the quantity to experiments which are accurate to eight digits for the electron and

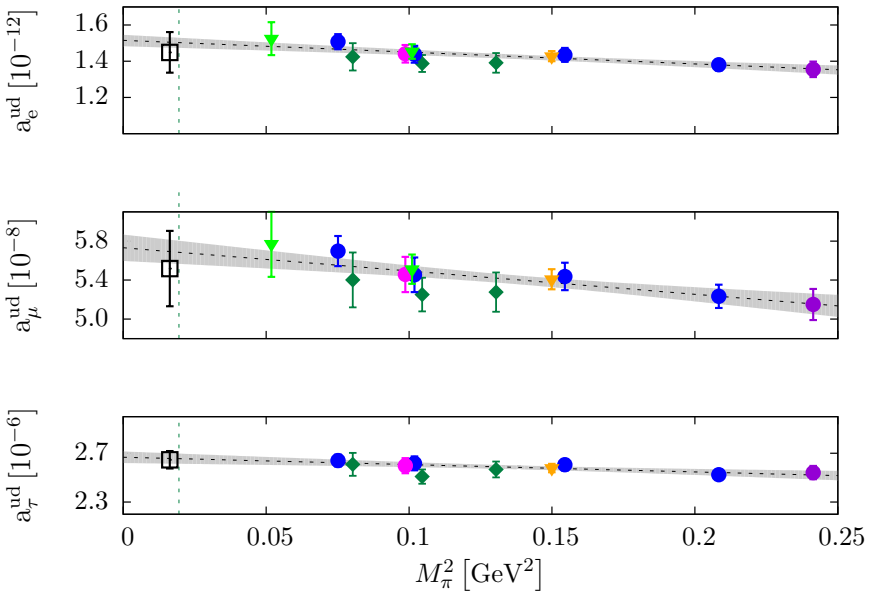

Figure 5. Comparison of the chiral extrapolation of the light quark contributions to the three lepton anomalous magnetic moments obtained from $N_f = 2+1+1$ simulations to the values at the physical value of the pion mass (black square). The dark green diamonds correspond to $a = 0.086$fm and $L = 2.8$fm and the circles to $a = 0.078$fm, the violet one stands for $L = 1.9$fm, the blue ones for $L = 2.5$fm, and the pink for $L = 3.7$fm. The orange triangle shows the value obtained for $a = 0.061$fm and $L = 1.9$fm and the light green triangle denotes $a = 0.061$fm and $L = 2.9$fm.

seven digits for the muon anomalous magnetic moments. Since the tau lepton has a very short lifetime $O(10^{-13}\text{seconds})$ there is presently no experimental result for its anomalous magnetic moment. Deriving the anomalous moment from field theory, one may, and does, employ an expansion in the electromagnetic and weak couplings but not in the strong coupling. The hadronic contribution is the given by

$$a_{\mathrm{l}}^{\mathrm{hvp}} = \alpha^2 \int_0^\infty \frac{dQ^2}{Q^2} w\left(\frac{Q^2}{m_{\mathrm{l}}^2}\right) \Pi_{\mathrm{R}}(Q^2)\ , \tag{2}$$

with $\Pi_{\mathrm{R}}(Q^2)$ the renormalised hadronic vacuum polarisation function and $w(x)$ a known function.

In Fig. 5 a comparison of the previous results in $N_{\mathrm{f}} = 2+1+1$ flavours at pion masses above the physical point and the new $N_{\mathrm{f}} = 2$ numbers is shown. The two results are consistent. Note that in this plot there is a significant variation of the number of flavours in the sea, the lattice volume, pion mass and the lattice spacing. A mutual agreement between these results is therefore not trivial and suggests that these systematic errors are under control.

4 Conclusion

The ability to simulate QCD on the lattice has progressed significantly over the last years, to the extent that we can now control all systematic effects coming from the finite volume, the non-physical quark masses and the finite lattice spacing to the level of per cent accuracies for a number of observables.

This is due to improved algorithms, computational strategies and codes which exploit the improved hardware resources. Of course challenges remain. Many observables are still not accessible to lattice calculations with the accuracies required to make an impact in the phenomenological analysis of high-energy physics data. And ever changing hardware will also pose new requirements on the algorithms and the software.

References

1. A. Ukawa, *Computational cost of full QCD simulations experienced by CP-PACS and JLQCD Collaborations*, Nucl. Phys. Proc. Suppl., **106**, 195–196, 2002, [,195(2002)].
2. M. Hasenbusch, *Speeding up the hybrid Monte Carlo algorithm for dynamical fermions*, Phys.Lett., **B519**, 177–182, 2001.
3. M. Hasenbusch and K. Jansen, *Speeding up lattice QCD simulations with clover improved Wilson fermions*, Nucl.Phys., **B659**, 299–320, 2003.
4. I. P. Omelyan, I. M. Mryglod, and R. Folk, *Symplectic analytically integrable decomposition algorithms: classification, derivation, and application to molecular dynamics, quantum and celestial mechanics simulations*, Computer Physics Communications, **151**, no. 3, 272 – 314, 2003.
5. M. Lüscher, *Local coherence and deflation of the low quark modes in lattice QCD*, JHEP, **0707**, 081, 2007.
6. A. Frommer, K. Kahl, S. Krieg, B. Leder, and M. Rottmann, *Adaptive Aggregation-Based Domain Decomposition Multigrid for the Lattice Wilson–Dirac Operator*, SIAM Journal on Scientific Computing, **36**, no. 4, A1581–A1608, 2014.
7. M. Lüscher, *Properties and uses of the Wilson flow in lattice QCD*, JHEP, **1008**, 071, 2010.
8. S. Schaefer, R. Sommer, and F. Virotta, *Critical slowing down and error analysis in lattice QCD simulations*, Nucl.Phys., **B845**, 93–119, 2011.
9. M. Lüscher and S. Schaefer, *Lattice QCD without topology barriers*, JHEP, **1107**, 036, 2011.
10. M. Lüscher and S. Schaefer, *Lattice QCD with open boundary conditions and twisted-mass reweighting*, Comput.Phys.Commun., **184**, 519–528, 2013.
11. A. Abdel-Rehim *et al.*, *Simulating QCD at the Physical Point with $N_f = 2$ Wilson Twisted Mass Fermions at Maximal Twist*, 2015.
12. M. Bruno *et al.*, *Simulation of QCD with $N_f = 2 + 1$ flavors of non-perturbatively improved Wilson fermions*, JHEP, **02**, 043, 2015.